The Kinetics of Carbonyl Formation in Asphalt

Meng Liu, K. M. Lunsford, R. R. Davison, C. J. Glover, and J. A. Bullin
Dept. of Chemical Engineering, Texas A&M University, College Station, TX 77843

The oxidation of asphalt is a major cause of pavement failure. The low-temperature oxidation kinetics of 14 asphalts are presented. At constant temperature and oxygen pressure, asphalt oxidation occurs in two stages: (1) a relatively rapid-rate period, followed by (2) a long period of constant rate. Activation energies for the constant-rate region vary from 64 to 109 kJ/mol, and reaction orders relative to oxygen pressure vary from 0.25 to 0.61. This variation in activation energy and reaction order leads to skepticism regarding the present practices of evaluating road-condition asphalt-hardening rates at a single elevated temperature and perhaps at an elevated pressure. The asphalts occur in essentially two groups, one at high values of both activation energy and reaction order and the other at low values of each. The data indicate the existence of an isokinetic temperature near 100°C. The degree of oxidation that occurs during the initial rapid-rate region varies inversely with the oxygen reaction order of the constant-rate region.

Introduction

Asphalt is a major by-product of the refining industry. About 28 million ton/yr are produced for use primarily in road construction and repair. An important factor in road life is the oxidation and subsequent hardening of the asphalt binder with age. Many accelerated aging tests have been devised in an attempt to rank asphalts according to their tendency to oxidize and harden. These are invariably run at elevated temperatures and sometimes at elevated pressures. A recent test developed by the Strategic Highway Research Program (SHRP) specifies the use of air at a pressure of 20 atm and at a temperature of 373 K.

Although many aging tests exist, there have been few studies of asphalt oxidation kinetics, and almost none to determine if the activation energies or oxygen reaction orders are different for different asphalts. This is an important practical question, for if asphalts are to be compared in tests run at temperatures and pressures significantly different from road conditions, there is a tacit assumption that all asphalts exhibit the same activation energy and reaction order.

Several authors have demonstrated that the formation of carbonyl-containing compounds in an asphalt as a result of oxidative aging changes the physical properties of the asphalt in a predictable way (Lee and Huang, 1973; Martin et al., 1990; Lau et al., 1992; Petersen et al., 1993). This relationship is different for different asphalts, but for each asphalt the change in carbonyl content, *CA*, is an excellent surrogate for the total oxidative changes and a predictor of the resulting changes in physical properties. This is partly explained by the fact that for each asphalt there is a linear relation between carbonyl growth and total oxygen increase, as seen in Figure 1 for two of the test asphalts.

Lau et al. (1992) showed that at 20-atm oxygen pressure and at temperatures from 333 to 366 K (140–200°F) the car-

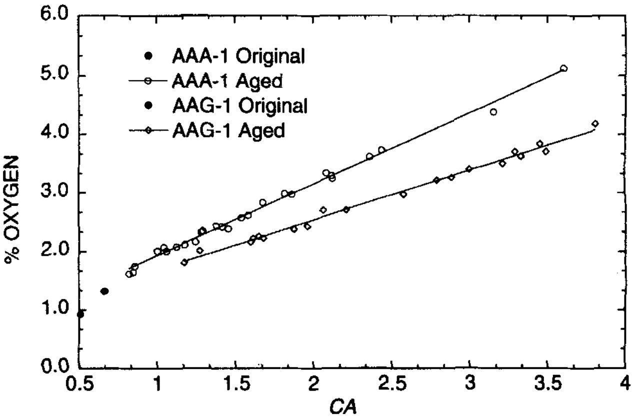

Figure 1. Oxygen percentage vs. carbonyl content for two POV-aged SHRP asphalts.

Aging temperatures 170°, 180°, and 190°F; aging pressures 0.2 atm and 20 atm.

Correspondence concerning this article should be addressed to C. J. Glover.

bonyl formation rate became constant after an initial more rapid rate region. These constant rates varied linearly with reciprocal absolute temperature in the usual Arrhenius form

$$r_{CA} = A'\exp(-E/RT). \qquad (1)$$

For the five asphalts studied, there appeared to be minor variations in the slopes of ln r_{CA} vs. $1/T$. In the present work, carbonyl formation kinetics are determined for a range of temperatures and pressures for 14 asphalts to determine definitely the effect of these variables on carbonyl formation rates. All rates are expressed in arbitrary carbonyl units as CA/d. These rates could be converted into units of percent oxygen per day using data such as those shown in Figure 1. The units are immaterial for the purposes of this study, and carbonyl is much easier to measure.

Experimental Design

This research was conducted in two phases. In the first phase, the same asphalts studied by Lau et al. (1992) were oxidized at 0.2, 2- and 20-atm oxygen and at 333.3, 344.4 and 355.5 K (140, 160 and 180°F). The second-phase study involved 10 asphalts with one, the Lau4, a repeat from the first phase. The rest of phase 2 material comprised two Texas asphalts (TX1 and TX2) and 7 asphalts from the SHRP project (AAA-1, AAD-1, AAF-1, AAG-1, AAM-1, AAB-1, AAS-1). The aging conditions used in this phase are listed in Table 1.

In the SHRP aging procedure, asphalts are first aged in the Thin-Film Oven Test (ASTM D-1754) to simulate hot-mix aging. To see if this made any difference, many of the second-phase samples were run following the equivalent Rolling Thin-Film Oven Test (ASTM D-2872). Many, but not all, were run in duplicate; that is, both virgin asphalt and oven-aged asphalt were run at the same condition.

The reaction equipment was the same as described by Lau, except that in phase 2, temperature control was improved by total immersion of the pressure oxygen vessel (POV) in a triethylene glycol bath. Asphalt samples weighing about 2 to 2.4 g were melted and placed in 4-cm × 7-cm aluminum trays. This gives a film thickness of 1 mm or less. Each POV holds 60–70 of these trays. For each asphalt a tray was removed every few days, depending on the temperature and pressure, with the maximum time ranging to 180 days at 333.3 K in the first phase. Oxygen content (Figure 1) was obtained using a Fisons EA 1108 CHNS-O Analyzer through direct oxygen measurement. Carbonyl content analysis was by infrared spectra using a Mattson Galaxy 5000 FT-IR and the attenuated total reflectance (ATR) method as described by Jemison et al. (1992).

Table 1. Aging Conditions Applied in the Phase-2 Experiments

Condition	Temperature	Pressure
*C*1	170°F (349.8 K)	20 atm
*C*2	180°F (355.5 K)	20 atm
*C*3	180°F (355.5 K)	10 atm
*C*4	190°F (360.9 K)	20 atm
*C*5	190°F (360.9 K)	0.2 atm
*C*6	200°F (366.5 K)	0.2 atm
*C*7	210°F (372.0 K)	0.2 atm

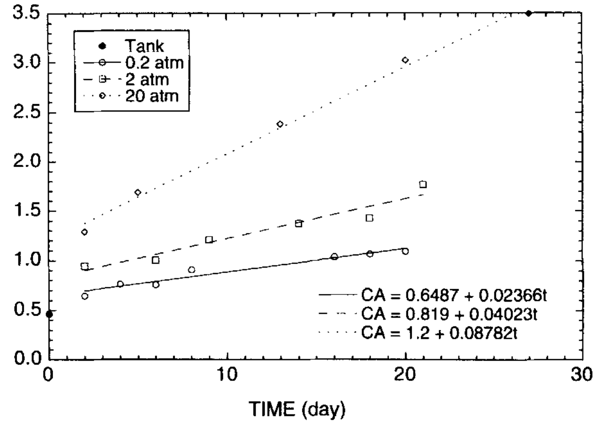

Figure 2. *CA* growth for tank and POV-aged Lau3 at 355.5 K and different oxygen pressures.

The integrated peak in the carbonyl region from 1,650 to 1,820 cm^{-1} was defined as the carbonyl area, CA, and was used to monitor the progress of oxidation.

Gas-phase diffusion was eliminated by using pure oxygen. Diffusion in the asphalt was eliminated by placing the exposed surface directly on the prism. Since the reflected rays only penetrate about one micron, this is essentially a surface measurement. Some analyses were also made by mixing the film before placing it on the prism. It was found that at 20 atm the results were indistinguishable from the surface measurements, and, since easier, the bulk measurements were used at this pressure.

Discussion of Phase-1 Results

As determined by Lau et al. (1992), the rates of carbonyl formation became constant for all five asphalts after an initial higher rate period. This is seen in Figure 2, where results at all three pressures and at 355.5 K are shown for one asphalt, and in Figure 3 where results for all three temperatures are shown at 2 atm. The intercept of the constant-rate portion regression line is defined as the initial jump, CA_0, while the slope of the line is the aging rate. From Figures 2

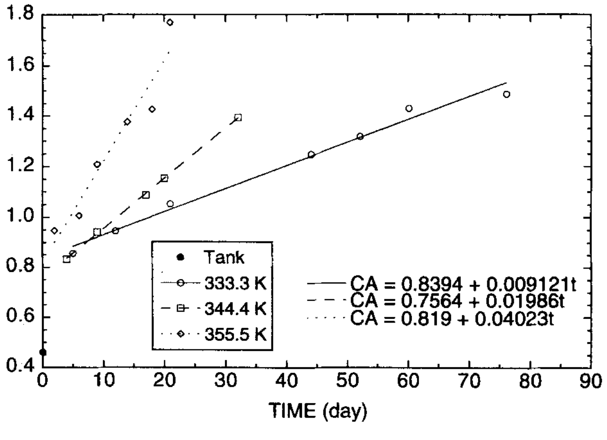

Figure 3. *CA* growth for tank and POV-aged Lau3 at 2 atm and different temperatures.

Table 2. *CA* Growth Rate for All Asphalts and POV Aging Conditions in the Phase-1 Experiments

Aging Condition		$r_{CA} \times 10^3$ (*CA*/day)				
Pres.	Temp.	Lau1	Lau2	Lau3	Lau4	Lau5
0.2 atm	333.3 K	3.24	3.73	4.75	4.19	3.66
	344.4 K	6.85	8.91	11.41	7.87	7.78
	355.5 K	18.66	21.32	23.66	19.73	18.62
2 atm	333.3 K	6.79	6.36	9.12	8.10	6.04
	344.4 K	14.55	15.74	19.86	13.92	14.80
	355.5 K	34.50	37.92	40.23	32.47	28.63
20 atm	333.3 K	12.34	11.46	18.58	12.40	10.95
	344.4 K	25.55	31.19	32.88	29.43	29.96
	355.5 K	67.02	78.21	87.82	60.18	56.64

and 3, it is observed that (1) the initial jump is pressure dependent and not temperature dependent, (2) aging rate increases with pressure, and (3) aging rate increases with temperature. Rate data for all phase 1 conditions are shown in Table 2 and $CA_0 - CA_{\text{tank}}$ in Table 3. Table 3 shows again that CA_0 is a function of pressure but, despite scatter, does not appear to be a function of temperature. Also, these conclusions are strongly supported by the phase-2 studies, which appear in the next section.

Figures 2 and 3 suggest that, as in classic kinetics, the aging rate can be expressed as

$$r_{CA} = AP^{\alpha}\exp(-E/RT), \qquad (2)$$

where A is the frequency factor, α is the reaction order with respect to oxygen pressure, and E is the activation energy. For this expression to be valid, it is necessary to verify that α is temperature independent and E is pressure independent.

Figure 4 is a plot of aging rates vs. oxygen pressures for all five asphalts at 344.4 K. Values at all temperatures are listed in Table 4. The scatter in α appears random, and we conclude that α is independent of temperature. An Arrhenius plot for all five asphalts at 0.2 atm is shown in Figure 5. The activation energy, E, is calculated from the slope, and values at all pressures are given in Table 5. Again, the variation appears random and we conclude that E is independent of pressure. These results justify the use of Eq. 2.

Equation 2 can be linearized by taking the natural logarithm of both sides

$$\ln r_{CA} = \ln A + \alpha \ln P - E/RT. \qquad (3)$$

Table 3. $CA_0 - CA_{\text{tank}}$ for All Asphalts and POV Aging Conditions in the Phase-1 Experiments

Aging Conditions		$CA_0 - CA_{\text{tank}}$ (*CA*)				
Pres.	Temp.	Lau1	Lau2	Lau3	Lau4	Lau5
0.2 atm	333.3 K	0.217	0.157	0.205	0.248	0.104
	344.4 K	0.202	0.180	0.176	0.271	0.142
	355.5 K	0.153	0.114	0.187	0.320	0.122
2 atm	333.3 K	0.278	0.334	0.377	0.413	0.248
	344.4 K	0.220	0.300	0.294	0.331	0.227
	355.5 K	0.295	0.276	0.357	0.352	0.290
20 atm	333.3 K	0.253	0.498	0.683	0.570	0.353
	344.4 K	0.438	0.548	0.920	0.616	0.376
	355.5 K	0.252	0.377	0.738	0.519	0.412

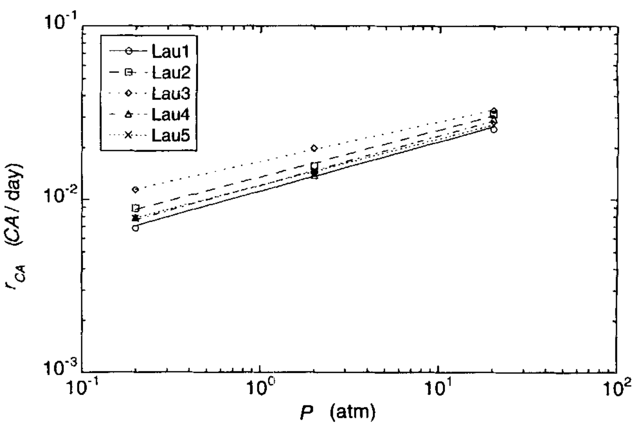

Figure 4. *CA* growth-rate dependence on pressure at 344.4 K for all POV-aged asphalts in the phase-1 experiments.

Table 4. α for All POV-Aged Asphalts at Different Temperatures in the Phase-1 Experiments*

	α				
Temp.	Lau1	Lau2	Lau3	Lau4	Lau5
333.3 K	0.290	0.244	0.296	0.236	0.238
344.4 K	0.286	0.272	0.230	0.286	0.270
355.5 K	0.278	0.282	0.285	0.242	0.242
Avg.	0.285	0.266	0.270	0.255	0.250

*Oxygen pressure from 0.2 to 20 atm.

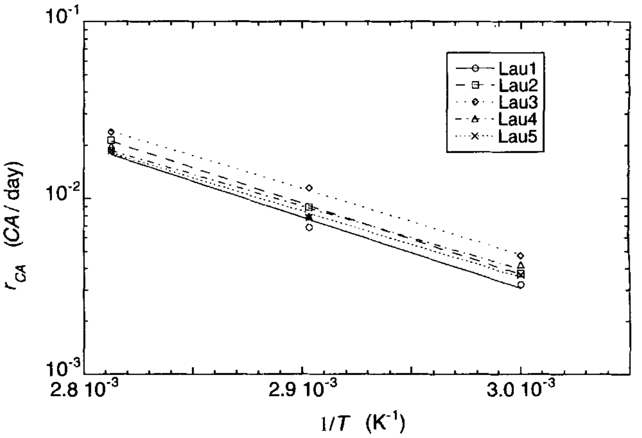

Figure 5. r_{CA} vs. $1/T$ at 0.2 atm for all POV-aged asphalts in the phase-1 experiments.

Table 5. *E* for All POV-Aged Asphalts at Different Pressures in the Phase-1 Experiments*

	E (kJ/mol)				
Pres.	Lau1	Lau2	Lau3	Lau4	Lau5
0.2 atm	77.5	77.2	71.2	68.5	72.0
2 atm	72.0	79.1	65.8	61.4	68.3
20 atm	74.8	85.1	68.6	70.1	72.9
Avg.	74.8	80.5	68.5	66.7	71.1

*Aging temperature from 333.3 to 355.5 K.

Table 6. Kinetic Model Parameters for All POV-Aged Asphalts in the Phase-1 Experiments

Asphalt	$\ln(A)$ $\ln(CA/\mathrm{d}\cdot\mathrm{atm}^{\alpha})$	E kJ/mol	α	Avg. % Error*
Lau1	21.71±2.60	74.8±7.4	0.285±0.036	7
Lau2	23.83±1.55	80.5±4.4	0.266±0.022	4
Lau3	19.86±2.67	68.6±7.6	0.270±0.037	7
Lau4	19.86±2.89	66.7±8.3	0.255±0.040	8
Lau5	20.42±1.77	71.1±5.1	0.250±0.025	5

$$^{*}\%\ \text{Error} = 100\sqrt{\sum \frac{1}{n}\left(\frac{\text{mea}-\text{cal}}{\text{mea}}\right)^{2}}.$$

This equation was used to perform a multivariable regression of r_{CA} as a function of T and P. Table 6 shows the estimated parameters. For each of the parameters, statistical methods were employed to obtain 95% confidence limit, and these are also shown in the table. The error of the estimated r_{CA} is also given. The percent errors are all under 10%.

The data in Table 6 show that a 95% confidence limit is roughly 15% of the value of the parameter. Unfortunately, the size of the confidence limit is such that it is difficult to conclude if the parameters are dependent on the asphalt source. Since the Arrhenius parameters describe the temperature dependence, and this is the most significant factor affecting the determination of r_{CA}, it appears that the Arrhenius parameters are probably composition dependent.

Discussion of Phase-2 Results

The study was greatly expanded to determine definitely if there are significant compositional effects in asphalt kinetics. Ten asphalts were aged at the conditions listed in Table 1. Table 7 shows the rates, and Table 8 shows the corresponding values of $CA_0 - CA_{\mathrm{tank}}$ for all 10 asphalts. Carbonyl growth with respect to aging time for three of the ten asphalts are shown in Figures 6 to 8. The data presented in Figure 6 are for one of the two asphalts that perhaps show some effect of oven aging on the subsequent POV aging, but only at 20 atm. We also see that the initial jump $CA_0 - CA_{\mathrm{tank}}$ is extremely small. The data in Figure 7 show no evidence of an oven-aging effect, but a larger pressure effect on CA_0 is evident. Figure 8 also shows no oven-test effect, but does show a very large pressure-dependent initial jump. In these runs, not all conditions were duplicated for both oven-aged and virgin material. Within the scatter of the data in Table 8, CA_0 appears temperature independent, and all but AAA-1 and AAD-1 show a definite pressure effect. For these two, $CA_0 - CA_{\mathrm{tank}}$ is negligible.

The constants in Eq. 3 determined by a multivariable regression for the phase-2 asphalts are listed in Table 9. Unlike

Table 7. *CA* Growth Rate for All POV-Aged Asphalts in the Phase-2 Experiments at all Conditions

	$r_{CA}\times 10^{3}$ (CA/d)						
Asphalt	$C1$	$C2$	$C3$	$C4$	$C5$	$C6$	$C7$
AAA-1	121.7	179.5		349.6	19.84	48.68	58.77
AAA-1 R*	114.5	181.9			16.29	49.12	54.90
AAD-1	133.3	223.5		403.9	22.53	43.69	60.01
AAD-1 R*	124.6	214.1			22.77	35.30	56.80
AAF-1	63.96	86.40		164.3	31.83	41.63	64.98
AAF-1 R*	65.84	88.55			32.83	37.75	61.61
AAG-1	74.66	102.0		163.3	41.41	60.17	87.57
AAG-1 R*	69.38	99.67			38.04	69.74	74.55
AAM-1	52.31	65.36		111.9	22.36	44.56	56.32
AAM-1 R*	50.66	62.15			28.30	45.26	59.33
AAB-1	68.77	132.3		222.2		58.19	80.39
AAB-1 R*	67.15	130.9	101.4	220.2		53.95	77.12
AAS-1	60.49			188.8			64.50
AAS-1 R*	58.19	105.1	86.59	197.8		46.17	64.72
TX1				229.4			85.39
TX1 R*	70.61	132.0	108.5	239.5		62.27	85.27
Lau4		108.0					
Lau4 R*	79.22	101.3	76.19	149.3		57.92	79.65
TX2		135.4					
TX2 R*	71.27	133.3	108.5	244.4		61.23	75.57

*Asphalt pretreated by Rolling Thin-Film Oven Test before aging under the conditions.

Table 8. $CA_0 - CA_{\mathrm{tank}}$ of All POV-Aged Asphalts in the Phase-2 Experiments at all Aging Conditions

	$CA_0 - CA_{\mathrm{tank}}$ (CA)						
Asphalt	$C1$	$C2$	$C3$	$C4$	$C5$	$C6$	$C7$
AAA-1	0.103	0.068		0.024	0.250	0.109	0.082
AAA-1 R*	0.092	−0.037			0.320	0.119	0.129
AAD-1	0.225	0.071		0.047	0.271	0.134	0.082
AAD-1 R*	0.253	0.040			0.292	0.304	0.150
AAF-1	0.782	0.771		0.742	0.336	0.385	0.279
AAF-1 R*	0.755	0.734			0.309	0.415	0.313
AAG-1	1.771	1.686		1.713	0.572	0.473	0.415
AAG-1 R*	1.801	1.694			0.630	0.405	0.503
AAM-1	0.780	0.839		0.811	0.402	0.281	0.309
AAM-1 R*	0.782	0.829			0.297	0.284	0.273
AAB-1	0.508	0.393		0.395		0.210	0.198
AAB-1 R*	0.533	0.412	0.358	0.383		0.259	0.223
AAS-1	0.404			0.342			0.206
AAS-1 R*	0.404	0.350	0.291	0.325		0.225	0.202
TX1				0.415			0.176
TX1 R*	0.447	0.352	0.356	0.361		0.171	0.190
Lau4		0.593					
Lau4 R*	0.501	0.643	0.549	0.706		0.252	0.267
TX2		0.365					
TX2 R*	0.371	0.348	0.310	0.280		0.188	0.185

*Asphalt pretreated by Rolling Thin-Film Oven Test before aging under the conditions.

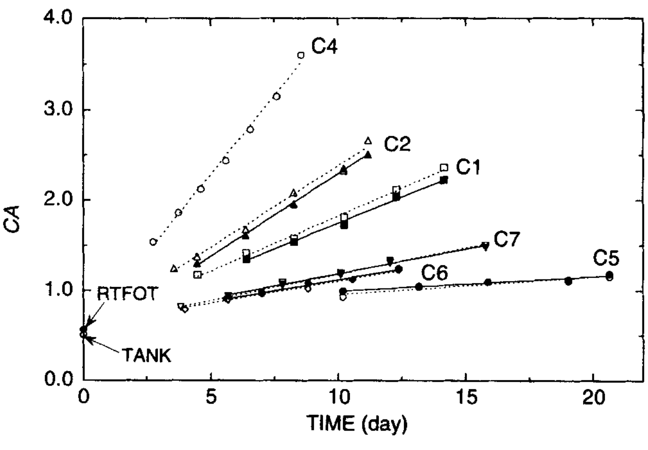

Figure 6. *CA* growth for tank, RTFOT-aged, and POV-aged SHRP AAA-1.

Solid: aged after pretreatment of Rolling Thin-Film Oven Test. Open: aged from tank, without pretreatment.

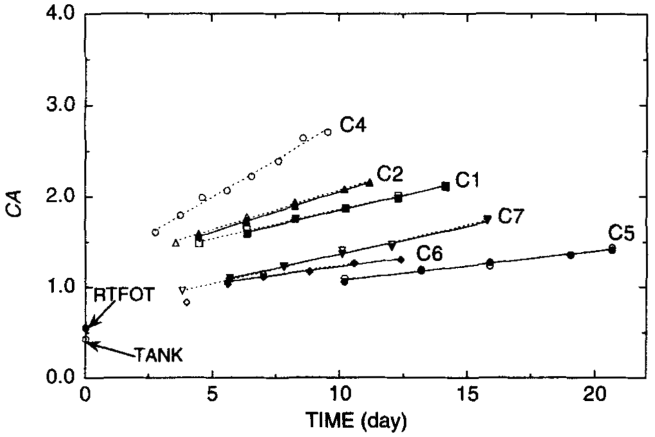

Figure 7. CA growth for tank, RTFOT-aged, and POV-aged SHRP AAF-1.

Solid: aged after pretreatment of Rolling Thin-Film Oven Test. Open: aged from tank, without pretreatment.

the phase 1 results, a much wider variation in reaction order, α, and activation energy, E, was obtained. The one duplicate asphalt, Lau4, yielded values very close to those previously obtained. We have in phase 1 a classic example of the statistical danger of small samples. Of the 14 asphalts tested in both phases, 7 have values of α between 0.25 and 0.29, with others ranging up to 0.61, yet all five of the asphalts tested by Lau and used in phase 1 lie in that narrow range. Similarly, the activation energies for the phase-1 asphalts ranged from about 67 to 81 kJ/mol, while the range of all 14 was 64 to 109. It is interesting that there seems to be distinct groupings of low α, low E asphalts, and high α, high E asphalts with no values of E between 81 and 100 and only one α between 0.29 and 0.42. The same kind of variation is seen in ln A.

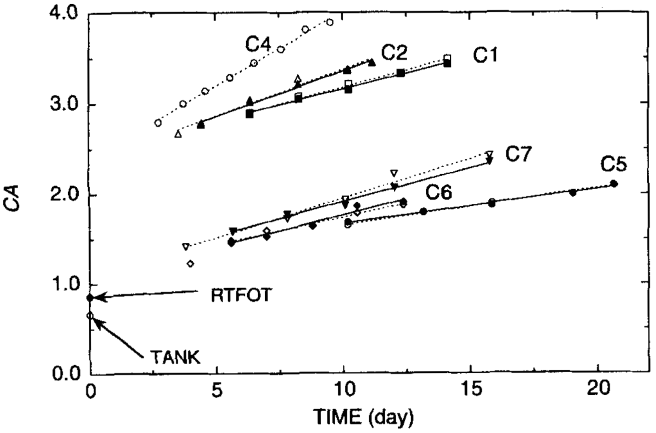

Figure 8. CA growth for tank, RTFOT-aged, and POV-aged SHRP AAG-1.

Solid: aged after pretreatment of Rolling Thin-Film Oven Test. Open: aged from tank, without pretreatment.

Table 9. Kinetic Model Parameters of All POV-Aged Asphalts Studied in the Phase-2 Experiments

Asphalt	ln A ln$(CA/\text{d}\cdot\text{atm}^{\alpha})$	E kJ/mol	α	Avg. % Error*
AAA-1	33.28 ± 10.86	108.5 ± 32.7	0.604 ± 0.099	16
AAD-1	30.59 ± 4.19	100.2 ± 12.6	0.611 ± 0.038	6
AAF-1	22.06 ± 5.92	75.1 ± 17.8	0.340 ± 0.054	9
AAG-1	20.71 ± 5.08	70.3 ± 15.3	0.279 ± 0.046	7
AAM-1	19.43 ± 4.67	67.5 ± 14.1	0.260 ± 0.042	7
AAB-1	31.60 ± 4.93	103.2 ± 14.9	0.426 ± 0.047	7
AAS-1	31.98 ± 5.58	105.0 ± 16.8	0.445 ± 0.052	6
TX1	31.29 ± 6.82	102.1 ± 20.6	0.421 ± 0.064	7
Lau4	18.64 ± 8.51	64.2 ± 25.6	0.272 ± 0.076	6
TX2	31.06 ± 13.06	101.5 ± 41.1	0.429 ± 0.122	9

*As defined in Table 6.

In Figure 9, ln A + α ln 0.2 (the value of E/RT, where ln $r_{CA} = 0$ for oxidation pressure of 0.2 atm) is plotted vs. E with remarkable linearity. This indicates that at 0.2-atm oxygen pressure there exists an isokinetic temperature (Boudart, 1991) where all 14 asphalts will exhibit nearly the same rate. From the fit in Figure 9, this temperature is calculated to be 370.8 K. In Figures 10 and 11, Arrhenius plots for the 10 phase-2 asphalts are shown corrected to 0.2 atm, and the rates do tend to converge in that region.

In Figure 12, we see the strong relation between E and α with only AAA-1 and AAD-1 appearing anomalous, but these two asphalts are alike in other respects. The confidence limits are higher for the second-phase runs because of fewer experimental conditions and differences in experimental design. However, the average errors are not much greater, and the good correlations in Figures 9 and 12, as well as the close agreement between the Lau4 results from each phase, give confidence in the results.

In Figures 9 and 12, we have distinguished between phase 1 and phase 2, which were run a year apart by different researchers. Both the narrow range of the phase 1 data as well as the general agreement with phase 2 results are evident.

Discussion of Activation Energies and Reaction Orders

There are a few activation energies published in the literature for asphalt oxidation. Whether these activation energies were measured for oxygen consumption or carbonyl formation is immaterial, because the linear relation between the two (see Figure 1) results in no effect on either E or α and only on ln A. Most of the published activation energies were obtained by measuring the rate of oxygen consumption at only

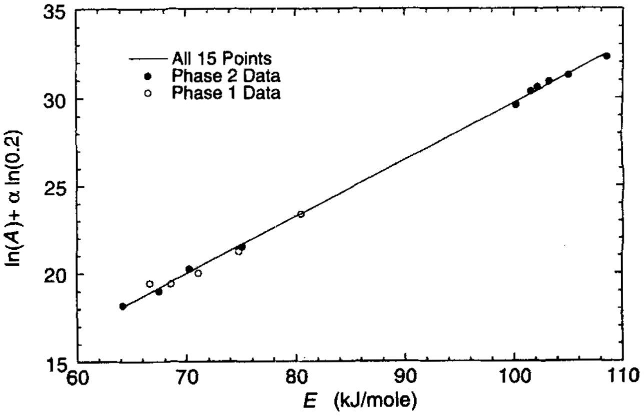

Figure 9. Isokinetic diagram for all 15 POV-aged asphalts.

Isokinetic temperature 370.8 K (270.8°F).

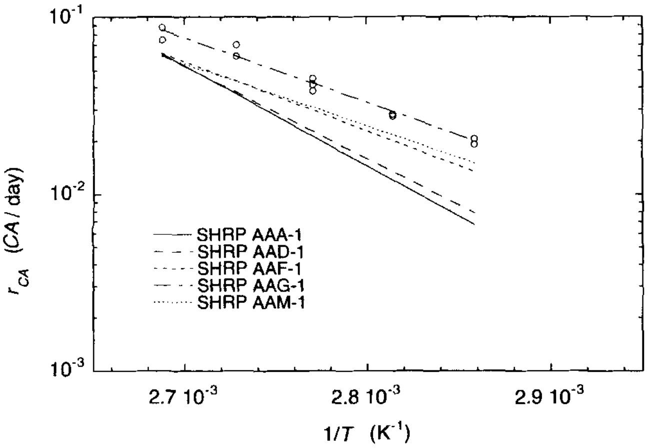

Figure 10. Arrhenius plot for five of the ten POV-aged asphalts in the phase-2 experiments.

two or three temperatures. Van Oort (1956) measured oxygen uptake at about 1 atm at 25, 50 and 75°C. Correcting for diffusion and assuming the reaction to be first order relative to oxygen pressure, he obtained a value of E of 100 kJ/mol. Blokker and van Hoorn (1959) gave the times required for 1 cm^3 of oxygen to absorb into a 200-micron film at 30 and 50°C. For the four asphalts they studied, the data yielded values of E from 55 to 79 kJ/mol. These authors also reported a value for α of 0.6, but gave no data. Dickinson and Nicholas (1949) and Dickinson et al. (1958) obtained values of E of 29 and 43 kJ/mol, but concluded these values contained diffusion effects. Verhasselt and Choquet (1991) reported a value of E for one asphalt of 87 kJ/mol measured between 343 and 373 K using carbonyl growth as the measurement.

All of these values, except for those recognized as being affected by diffusion, fall in the range of the present study. It should be pointed out, however, that several and perhaps all of them are based on rates measured totally or in part in the initial rapid-rate region and may well be different from values calculated in the constant-rate region. The single value given for the reaction order of 0.6 is at the upper limit of values obtained in this work. Again, it is quite possible that it was measured in the initial-rate region in which the pressure effect is quite different.

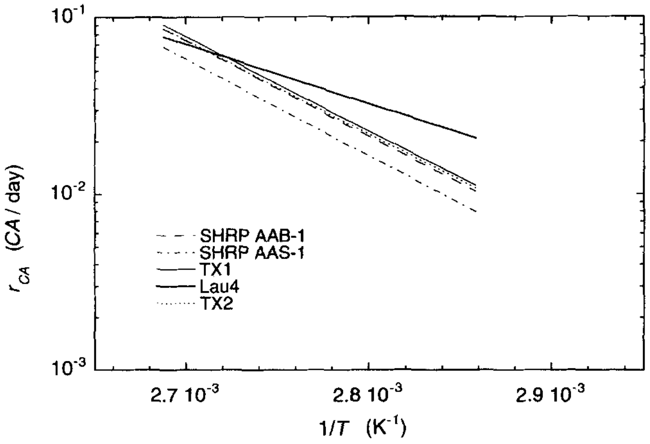

Figure 11. Arrhenius plot for five of the ten POV-aged asphalts in the phase-2 experiments.

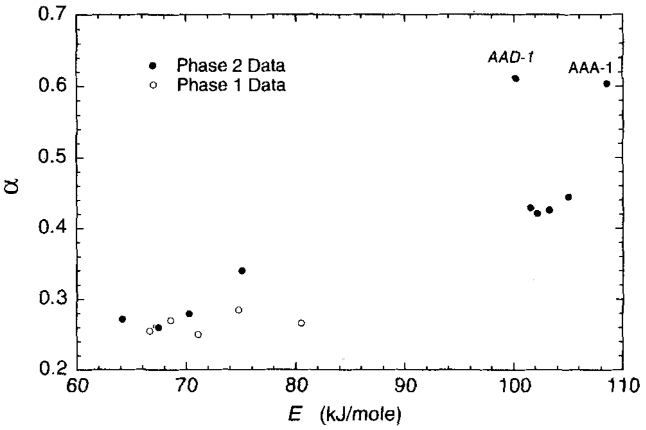

Figure 12. Reaction order vs. activation energy for all 15 POV-aged asphalts.

Initial Rapid-Rate Region

As was previously shown, the initial jump of the rapid-rate region, CA_0, and thus $CA_0 - CA_{\text{tank}}$, is not a function of reaction temperature but generally increases with reaction pressure. Also, Tables 8 and 3 show that asphalts with larger reaction orders α (e.g., AAA-1 and AAD-1) have smaller initial jumps, compared to those with lower α (e.g., AAF-1, AAG-1, AAM-1, and Lau4). This is particularly clear for the 20-atm data.

To evaluate the initial rapid-rate region, it was assumed that the pressure effect could be represented by

$$CA_0 - CA_{\text{tank}} = \beta P^{\gamma}. \tag{4}$$

All values of $CA_0 - CA_{\text{tank}}$ were used to fit β and γ, and the results are given in Table 10. For asphalts AAA-1 and AAD-1, the pressure effects are negligible and were calculated to be negative, but this is probably an error. Some of these values are calculated from only two data points. The constant β does not vary much, but γ is plotted vs. α in Figure 13, and surprisingly the pressure effect on CA_0 varies inversely with α, the reaction order with respect to oxygen pressure in the constant-rate region.

Table 10. β and γ Values of All Asphalts in the Phase-1 and Phase-2 Experiments*

	AAA-1	AAD-1	AAF-1	AAG-1	AAM-1
β	0.1102	0.1738	0.4492	0.7717	0.4312
γ	−0.2631	−0.1047	0.1741	0.2700	0.2097
	AAB-1	AAS-1	TX1	Lau4†	TX2
β	0.2755	0.2473	0.2361	0.3514	0.2300
γ	0.1383	0.1065	0.1699	0.1881	0.1305
	Lau1	Lau2	Lau3	Lau4‡	Lau5
β	0.2330	0.2340	0.2987	0.3481	0.1938
γ	0.1079	0.2498	0.3078	0.1536	0.2449

*$CA_0 - CA_{\text{tank}} = \beta P^{\gamma}$.
†By data of the phase-2 experiments.
‡By data of the phase-1 experiments.

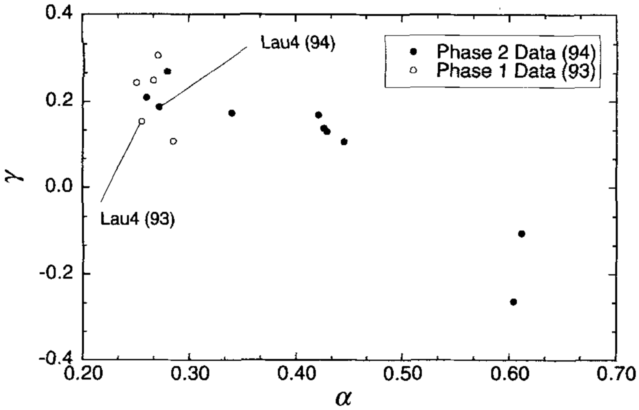

Figure 13. Initial jump pressure dependence factor γ vs. reaction order α.

(γ defined in Eq. 4).

Implications of the Results

The results of this work have profound significance in the development of a reliable aging test, as well as in the evaluation of asphalt-binder quality.

The fact that each asphalt has a specific set of kinetic parameters gives a guidance in developing a reliable aging test. Data in Table 9 show that asphalts from different sources may exhibit far different reaction orders and activation energies. Therefore, the relative aging rates that exist at one temperature and pressure may be reversed at another temperature and/or pressure. Any test using the information of only one aging experiment performed at a single elevated temperature and/or elevated pressure is not reliable. Furthermore, if the aging experiment is conducted within the initial rapid-rate region, the resulting relative rates also cannot represent the constant-rate-period relative rates that are relevant in the pavement. Based on this work, we conclude that a reliable aging test can only be conducted by running aging experiments at multiple temperatures and/or pressures to measure the kinetic parameters. The kinetic parameters can then be used to determine the aging rates at road conditions. The optimum protocol for such a testing procedure is yet to be established.

The differences between the kinetic parameters also indicate that aging characteristics are an important part of asphalt binder quality. Since the asphalts have an isokinetic temperature near 100°C, those with higher activation energies will have a lower oxidation rate at road conditions. Also, a small initial jump is desirable. On the other hand, as shown in Figures 12 and 13, the reaction order α, the activation energy E, and the initial jump pressure dependence factor γ are closely correlated. Since the kinetic parameters should be a manifestation of the chemical compositions of the asphalts, improvements in aging quality can be realized through compositional manipulations. The compositional dependence of the activation energy, reaction order, and initial jump is currently under investigation. Further results may yield techniques to manufacture asphalts with superior aging characteristics.

Finally, the isokinetic phenomenon as shown in Figure 9 is remarkable, and of fundamental significance. Boudart (1991) reported an isokinetic diagram for hydrocarbon cracking (C_3–C_6). By contrast, asphalt is a very complex petroleum residue consisting of thousands of compounds of much higher carbon number and widely varying functionalities. The existence of the isokinetic phenomenon in such a material is likely to be a valuable observation for understanding and describing the aging mechanism.

Conclusions

When asphalts are oxidized at constant oxygen pressure and constant temperature in the absence of diffusion, the carbonyl growth undergoes a period of rapid growth and then a lengthy period of constant rate. The kinetics of the constant-rate region are represented by Eq. 2, with both E and α being asphalt dependent and strongly cross-correlated in that generally high values of E accompany high values of α.

The initial jump, CA_0, is also highly asphalt dependent and is pressure dependent according to Eq. 4, but correlates inversely with the constant-rate reaction order. From these results it is apparent that any attempt to use relative asphalt-aging rates at elevated temperatures and pressures and to assume they represent relative rates at road conditions could be highly misleading.

Acknowledgments

Support for this work came from the Texas Department of Transportation (TxDOT), in cooperation with the U.S. Department of Transportation, and the Federal Highway Administration (FHWA). This work also supported by the U.S. Department of Energy (DOE), Assistant Secretary for Energy Efficiency and Renewable Energy, under DOE Albuquerque Operation Office Cooperative Agreement DE-FC04-93AL94460. The technical contributions of Mrs. Ann Ferry are greatly appreciated.

The contents of this article reflect the views of the authors who are responsible for the facts and accuracy of the data presented. The contents do not necessarily reflect the official views or policies of the Federal Highway Administration, the Texas Department of Transportation, or the U.S. Department of Energy. This report does not constitute a standard, specification, or regulation.

Notation

A' = Arrhenius constant in Eq. 1, CA/d
CA_{tank} = carbonyl content of virgin asphalt
P = oxygen pressure, atm
R = universal gas constant
T = temperature, K
β = model parameter in Eq. 4
γ = model parameter in Eq. 4

Literature Cited

Blokker, P. C., and H. van Hoorn, "Durability of Bitumen in Theory and Practice," *Proc. World Petroleum Cong.*, 417 (1959).

Boudart, M., *Kinetics of Chemical Process*, Butterworth-Heinemann, Stoneham, MA (1991).

Dickinson, E. J., and J. H. Nicholas, "The Reaction of Oxygen with Tar Oils," *Road Res. Tech.*, No. 16, 1 (1949).

Dickinson, E. J., J. H. Nicholas, and S. Boas-Traube, "Physical Factors Affecting the Absorption of Oxygen by Thin Film of Bitumen Road Binders," *J. Appl. Chem.*, **8**, 673 (1958).

Jemison, H. B., B. L. Burr, R. R. Davison, J. A. Bullin, and C. J. Glover, "Application and Use of the ATR, FT-IR Method to Asphalt Aging Studies," *Fuel Sci. Technol.*, **10**, 795 (1992).

Lau, C. K., K. M. Lunsford, C. J. Glover, R. R. Davison, and J. A. Bullin, "Reaction Rates and Hardening Susceptibilities as Determined from POV Aging of Asphalts," *Trans. Res. Rec.*, **1342**, 50 (1992).

Lee, D. Y., and R. J. Huang, "Weathering of Asphalts as Characterized by Infrared Multiple Internal Reflection Spectra," *Anal. Chem.*, **46**, 2242 (1973).

Martin, K. L., R. R. Davison, C. J. Glover, and J. A. Bullin, "Asphalt Aging in Texas Roads and Test Sections," *Trans. Res. Rec.*, **1269**, 9 (1990).

Petersen, J. C., J. F. Branthaver, R. E. Robertson, P. M. Harnsberger, J. J. Duvall, and E. K. Ensley, "Effects of Physicochemical Factors on Asphalt Oxidation Kinetics," *Trans. Res. Rec.*, **1391**, 1 (1993).

Van Oort, W. P., "Durability of Asphalt, Its Aging in the Dark," *Ind. Eng. Chem.*, **48**, 1196 (1956).

Verhasselt, A. F., and F. S. Choquet, "A New Approach to Studying the Kinetics of Bitumen Aging," *Proc. Int. Symp. Chemistry of Bitumens*, Vol. II, Rome, Italy, p. 686 (June 5–8, 1991).

Manuscript received Apr. 5, 1995, and revision received June 23, 1995.